Self-Association of Hydroxypropylcellulose in Water

Jun Gao, George Haidar, Xihua Lu, and Zhibing Hu*

Departments of Physics, Chemistry and Materials Science, University of North Texas, Denton, Texas 76203

Received September 21, 2000; Revised Manuscript Received January 19, 2001

ABSTRACT: The association of hydroxypropylcellulose (HPC) chains above their lower critical solution temperature (LCST, ∼41 °C) leads to metastable nanosphere aggregates instead of precipitation. Laser light scattering (LLS) measurements revealed that the size of the aggregates is dependent not only on temperature and HPC concentration but also on heating history. There existed a narrow temperature range from ∼41 to ∼44 °C in which narrowly distributed metastable nanospheres formed in a few minutes and lasted for a few days without changing their sizes and molar masses. Increasing temperature in this range and increasing HPC concentration resulted in larger and denser nanosphere aggregates. In situ cross-linking of self-associated HPC chains was performed in a LLS sample cuvette at 42 °C using divinyl sulfone as a cross-linker. Formation of HPC gel microspheres was monitored by LLS and demonstrated by allowing the gel microspheres to swell and shrink at temperatures below and above the LCST, respectively.

Introduction

Self-association is a well-known self-assembling phenomenon often found in diblock or triblock copolymer/solvent systems[1−12] where the selective solvent to specific polymer block(s) can lead to the formation of nanoparticles of chain aggregates without precipitation. Recently, it is of interest to use self-association for drug loading and controlled delivery.[13−15]

In almost all the methods of polymer nanoparticle or microgel formation, one can always find some stable factors that either decrease the Gibbs energy of the systems that have large surface areas or provide kinetic barriers to prevent particles from aggregation. Sometimes the stable factors are obvious. For example, in emulsion polymerization, adding a surfactant tremendously decreases the surface energy, while in surfactant-free emulsion polymerization, the ionic groups arising from ionic initiators often provide electrostatic repulsion to stabilize nanoparticle dispersions.[16,17] Sometimes, however, the stable factors may not be so obvious, especially for neutral homopolymers.

Wu and Zhou[18] observed the coil-to-globule phase transition of single neutral poly(*N*-isopropylacrylamide) (PNIPAM) homopolymer chains in extremely dilute water systems when the temperature increased above the θ temperature. They also found[19] that in more concentrated (1×10^{-5}−1×10^{-3} g/cm^3) solutions the association PNIPAM chains above their lower critical solution temperature (LCST, ∼32) leads to stable aggregates instead of the expected precipitation. In these processes, chain collapse accompanied chain association, forming very quickly stable aggregates of different sizes at different temperatures and concentrations. On the other hand, Ding and Liu[20] studied the growth and morphology change of diblock copolymer particles in solvent−nonsolvent systems before precipitation using microscopy. It is reasonable to rationalize that, for other polymer chains containing both hydrophobic and hydrophilic portions, changing the properties of the solvent may induce self-association, leading to the formation of nanoparticle aggregates.

* To whom correspondence should be addressed

In this work, we demonstrated that hydroxypropylcellulose (HPC), a kind of alkyl-substituted cellulose derivatives[21−24] possessing the LCST (∼41 °C for dilute concentration of $\sim 1 \times 10^{-4}$ g/cm^3) in water, similar to the PNIPAM, can self-associate at $T >$ LCST and form metastable nanoparticle aggregates. Heating a dilute HPC water solution to temperatures only a couple of degrees higher than LCST can create a bright bluish tint very abruptly, showing the nanoparticle formation via chain association. We further cross-linked self-associated HPC chain nanoparticles to obtain narrowly distributed surfactant-free HPC microgels.[25] HPC gels comprise natural cellulose ether macromolecules that have been approved by the United States Food and Drug Administration (FDA) and thus have significant practical advantage over most synthetic gels that are made from carcinogenic or teratogenic monomers. Bulk HPC hydrogels and its derivatives with various forms including homogeneous gel, porous gel, and gel beads have been studied before.[26−29] However, it was the first time to exploit the property of LCST to form HPC nanoparticles and then to cross-link them into gel nanospheres. We have also used the similar scheme (by adding surfactant) to synthesize HPC gel nanospheres[30] with different particle sizes and used these gel nanospheres as building blocks to form gel nanoparticle networks.[31]

Experimental Section

Materials. Hydroxypropylcellulose (HPC) (nominal M_w of 1×10^5 g/mol), divinyl sulfone (DVS), and NaOH were purchased from Aldrich Chemical Co. (all are reagent grade) and used as received. Distilled and deionized water (resistance of 18 MΩ·cm) was used throughout. A 1.00 wt % HPC stock solution was prepared by dissolving HPC in water under gentle stirring for 1 week to ensure thoroughly dissolved. A 0.5 μm Millipore (Millex LCR25) filter was used to clarify the dilute LLS sample solutions. Ultracentrifugation was used to make clarification of the concentrated ones.

Gelation. Divinyl sulfone (DVS) was used to chemically cross-link HPC chains by an addition reaction with hydroxyl groups on HPC chains, saturating the carbon−carbon double bonds on DVS. At pH of 12−13, the reaction can lead to either

10.1021/ma001631g CCC: $20.00
Published on Web 03/02/2001

a uniform or a porous bulk HPC hydrogel, depending on whether a lower or a higher temperature (than LCST) is used. In our work, we first made use of the self-association of HPC chains at temperatures higher than LCST to form nanoparticles of HPC chain aggregates and then started cross-linking (both inter and intra) of HPC chains inside each nanoparticle to obtain HPC gel nanospheres.

Laser Light Scattering (LLS). A commercial LLS spectrometer (ALV/DLS/SLS-5000) equipped with an ALV-5000 digital time correlator was used with a helium−neon laser (Uniphase 1145P, output power of 22 mW and wavelength of 632.8 nm) as the light source. The incident light was vertically polarized with respect to the scattering plane, and the light intensity was regulated with a beam attenuator (Newport M-925B). The scattered light was conducted through a thin (∼100 μm in diameter) optic fiber leading to an active quenched avalanche photodiode (APD), the detector. As a result, the coherent factor β in dynamic laser light scattering was 0.98 for our instrument. The avalanche photodiode had a sensitivity 2 orders of magnitude higher than that of a normal photon multiplier (PM) tube, while its dark count increased no more than 10 times, so that a 22 mW laser could have a measured count rate (scattered intensity) similar to a 400 mW laser for a normal PM tube.

In static light scattering (SLS), the angular and concentration dependence of the excess Rayleigh ratio $R_{vv}(q)$ of dilute polymer solutions or nanoparticle dispersions is measured. $R_{vv}(q)$ is related to the weight-average molar mass M_w, the second virial coefficient A_2, and the z-average root-mean-square radius of gyration $\langle R_g^2\rangle_z^{1/2}$ (or simply $\langle R_g\rangle$) by[32]

$$\frac{KC}{R_{vv}(q)} \cong \frac{1}{M_w}\left(1 + \frac{1}{3}\langle R_g^2\rangle q^2\right) + 2A_2C \qquad (1)$$

where $K = 4\pi^2 n^2 (dn/dC)^2/(N_A\lambda_0^4)$ and $q = (4\pi n/\lambda_0)\sin(\theta/2)$ with N_A, n, C, λ_0, and θ being Avegadro's constant, the solvent refractive index, the solid concentration (g/cm^3 or g/g), the light wavelength in the vacuum, and the scattering angle, respectively. The dn/dC value of HPC in water was taken as 0.164 cm^3/g as found in ref 33 without wavelength correction so that the molar masses obtained in our measurements are the apparent values. It is also noted that in our study the concentration (typically 5×10^{-5} g/cm^3) is very low and A_2 is small so that the extrapolation to zero concentration is not necessary. With the same dilute sample, we could perform DLS and SLS measurements in turns. In dynamic light scattering (DLS),[32,34] the Laplace inversion or cumulant analysis of the intensity−intensity−time correlation function resulted in the translational diffusion coefficient distribution $G(D)$ or further to the hydrodynamic radius distribution $f(R_h)$ by using the Stokes−Einstein equation, $R_h = k_BT/6\pi\eta D$, where k_B, η, and T are the Boltzmann constant, the solvent viscosity, and the absolute temperature, respectively. The DLS measurements were carried out at angle of 20°.

Results and Discussion

Figure 1 shows the Zimm plot of HPC chains in water at 25 °C. On the basis of eq 1, we were able to obtain M_w (7.3×10^4 g/mol), $\langle R_g\rangle = 36$ nm, and $A_2 = 9.0 \times 10^{-4}$ mol·cm^3/g) from the extrapolation of $[KC/R_{vv}(q)]_{q\to0,C\to0}$, $[KC/R_{vv}(q)]_{C\to0}$ vs q and $[KC/R_{vv}(q)]_{q\to0}$ vs C. For either very small molecules or very large chain aggregates (e.g., the bottom row in Table 3), it is difficult to get accurate values of $\langle R_g\rangle$ from SLS. In these two extreme cases, the estimated relative error of $\langle R_g\rangle$ is about 30% of their average values.

As expected, no aggregation happened, and HPC chains were in their random-coil states, as can be seen by the coherent values of measured and nominal M_w and the ratio of $\langle R_g\rangle/\langle R_h\rangle$ (where $\langle R_h\rangle$ is the z-average hydrodynamic radius) close to 1.5 (see Table 1). The positive value of A_2 shows that water is a good solvent for the HPC at room temperature.

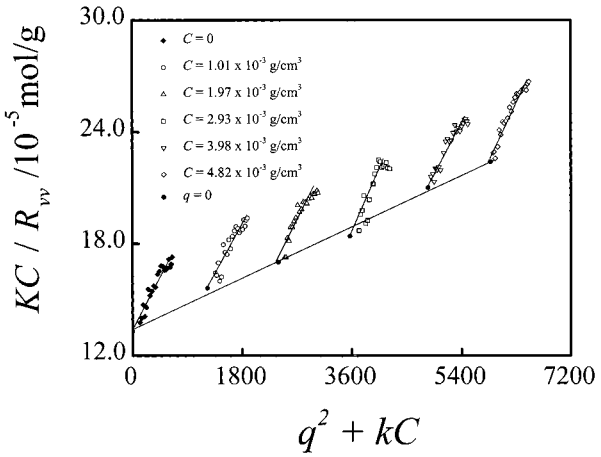

Figure 1. Zimm plot of HPC chains in water at 25.0 °C, where the concentration of HPC ranges from 1.01×10^{-3} to 4.82×10^{-3} g/cm^3.

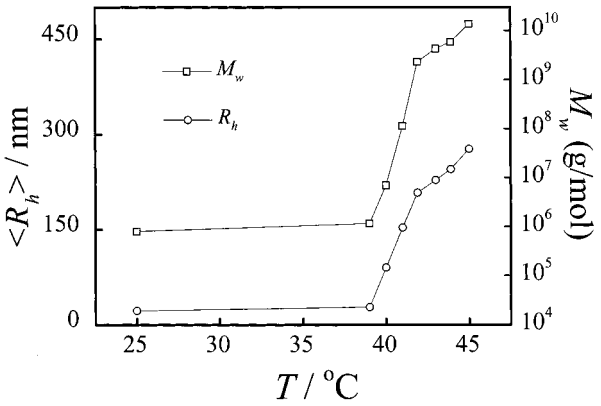

Figure 2. Temperature dependence of the average hydrodynamic radius $\langle R_h\rangle$ and the molar mass M_w of HPC chains or aggregates in the multistep heating, where the HPC concentration is 5.15×10^{-5} g/cm^3.

Table 1. Temperature Dependence of HPC Aggregates in Multistep Heating, Where the Concentration of HPC is 5.15×10^{-5} g/cm^3

T (°C)	$\langle R_g\rangle$ (nm)	$\langle R_h\rangle$ (nm)	$\langle R_g\rangle/\langle R_h\rangle$	M_w (g/mol)	ρ (g/cm^3)
25.1	36	22	1.6	8.0×10^4	
39.0	43	28	1.5	1.2×10^5	
40.0	67	90	0.74	7.0×10^6	
41.0	105	153	0.69	1.1×10^8	0.013
42.0	149	208	0.72	2.3×10^9	0.10
43.0	164	228	0.72	4.3×10^9	0.15
43.9	190	245	0.77	5.8×10^9	0.21
45.0	194	277	0.70	1.4×10^{10}	0.25

Figure 2 shows both DLS and SLS results of a multistep heating from 25 to 45 °C for a dilute HPC solution with concentration of 5.15×10^{-5} g/cm^3. The sample reached its stable/metastable state at each temperature in 10−30 min. Repeat measurements were performed at each temperature for more than 1 h to ensure the reliable data. Figure 3 further shows the related hydrodynamic radius distribution of either HPC chain coils or aggregates at different temperatures. It can be seen that at temperatures lower than 39 °C HPC chains existed in their single chain coil states with a broad hydrodynamic radius distribution (open circles in upper part of Figure 3). As the temperature increased to 39 °C, water became a relatively poor solvent, and HPC chains began to feel the hydrophobic attraction of

Table 2. Fluctuation Ranges of the Particle Size, the Molar Mass, and the Density of the Aggregates at 42 and 44 °C, Showing the Kinetic Stability of HPC Aggregates, Where the Concentration of HPC is 5.15×10^{-5} g/cm³

T range (°C)	duration (h)	$\langle R_g \rangle$ (nm)	$\langle R_h \rangle$ (nm)	$\langle R_g \rangle / \langle R_h \rangle$	M_w (g/mol)	ρ (g/cm³)
41.85−41.95	48	88−95 ⟨92⟩	132−138 ⟨135⟩	0.68	4.5×10^8−5.2×10^8	0.072−0.084
43.85−44.01	30	103−129 ⟨116⟩	166−172 ⟨168⟩	0.69	2.2×10^9−2.8×10^9	0.18−0.22
41.81−42.03	95	79−92 ⟨87⟩	152−161 ⟨155⟩	0.56	5.5×10^8−6.2×10^8	0.059−0.066

[a] Note: the $\langle R_g \rangle$ and $\langle R_h \rangle$ data inside "⟨ ⟩" are the most probable values in the respective temperature ranges.

Table 3. In-Situ Cross-Linking of HPC Aggregates into HPC Gel Microspheres, Where the Concentration of HPC is 5.15×10^{-5} g/cm³

	T (°C)	$\langle R_h \rangle$ (nm)	$\langle R_g \rangle$ (nm)	M_w (g/mol)	ρ (g/cm³)
HPC	42	135	92	4.5×10^8	0.07
HPC + DVS	41.8	125	60	4.5×10^8	0.09
HPC + DVS + NaOH	41.8	340	260	2.3×10^{10}	0.23
	25.0	580	400	2.1×10^{10}	0.04
	41.8[a]	320	360	2.5×10^{10}	0.30

[a] The second time the sample was heated to 41.8 °C.

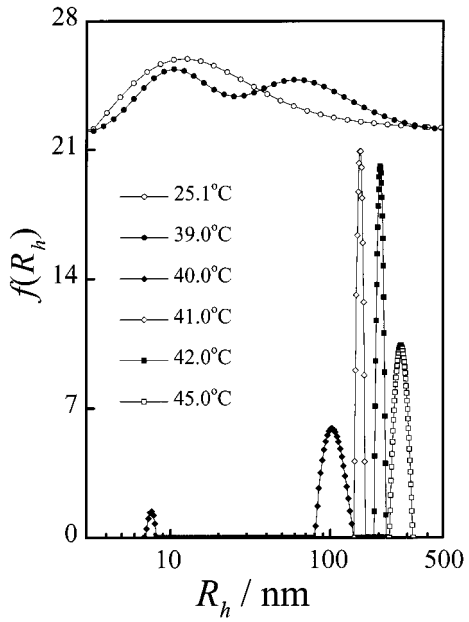

Figure 3. Hydrodynamic radius distribution of HPC chains or aggregates at different temperatures in multistep heating, where the HPC concentration is 5.15×10^{-5} g/cm³. The $f(R_h)$ at 25.1 and 39.0 °C is enlarged by multiplying 5, and the curves shifted upward 22 for better visual effect.

each other and showed a trace of association (solid circles). Note that $f(R_h)$ obtained from DLS was z-averaged, which means that, at this temperature, only a very small fraction of the HPC chains formed loose associates containing several chains, and most of the HPC chains were still in their dispersed single chain states. As a result, two partly merged peaks appeared, and $\langle R_h \rangle$ and M_w slightly increased (Figure 2). $\langle R_g \rangle / \langle R_h \rangle$ remained ~1.5 (Table 1).

At 40 °C, more HPC chains associated together as the solvent became poorer. However, there were some HPC chains that were in single-chain states as evidenced by the small (solid diamonds) peak on the left side of Figure 3. While both $\langle R_h \rangle$ and M_w increased, M_w was much more sensitive to the association/aggregation (Figure 2). The association of HPC chains led to the loose (instead of compact) aggregates, and the R_h distribution (40 °C, right side of solid diamonds peak in Figure 3) was not as narrow as that at higher temperatures (41 °C, open diamonds in Figure 3).

In the temperature range from 41.0 to 44.0 °C, very narrowly distributed nanoparticles of HPC aggregates formed (see open diamonds and solid squares in Figure 3 for HPC nanoparticles at 41 and 42 °C, respectively). As the temperature increased in this range, the size and the density (Table 1) of the aggregates increased, and M_w increased sharply. This indicates that under stronger driving force at higher temperature more HPC chains associated to form larger and denser particles. $\langle R_g \rangle / \langle R_h \rangle$ ratios in Table 1 are close to 0.774, the value for uniform nondraining spheres, indicating that the aggregates were uniform nanospheres.

As the temperature increased above 45.0 °C (open squares in Figure 3 and Table 1), even larger and denser particles formed. The aggregates tended to lose their kinetic stability, leading to broader distribution of R_h. The aggregates precipitated by the gravity at temperatures above 50 °C. It should be mentioned that more concentrated HPC solutions tend to precipitate at lower temperatures.

The self-association of polymer chains is related to a polymer phase separation process, which has been extensively studied in the past decades.[35,36] In the association involving particle nucleation and growth, the process can last as long as 1 week, as Ding and Liu[20] observed in their microscopy study. On the other hand, Wu and the co-workers[37−39] observed very fast (in seconds) nanoparticle formation via chain association when they dispersed a block copolymer chain solution into a secondary poor solvent. In our case, the HPC is a nonionic macromolecule possessing LCST in water like PNIPAM. Both macromolecular chains can form metastable nanospheres of aggregates in water by self-association of the chains in a suitable temperature range higher than their respective LCST. The driving force for the phase separation, resulting in both interchain association and intrachain collapse, is the hydrophobic attraction between hydrophobic moieties of the macromolecular chains when water becomes a poor solvent at $T >$ LCST. Intrachain collapse and interchain association are competitive. In extremely dilute ($\leq 10^{-7}$ g/cm³) solution, intrachain collapse is dominant and can lead to the formation of single-chain globules,[18] whereas in dilute or semidilute solution, interchain association is overwhelming and contributes to the formation of chain aggregates.

It is known that in both PNIPAM and HPC chains there are hydrophilic groups of either (−CONH−) or (−OH). The hydrogen bonds between water and these groups make both macromolecules soluble in water at room temperature. The weakening of the hydrogen bonds with increasing temperature may lead to the aggregation of the macromolecular chains when hydrophilic attraction between water and macromolecular chains could not counteract the interchain hydrophobic

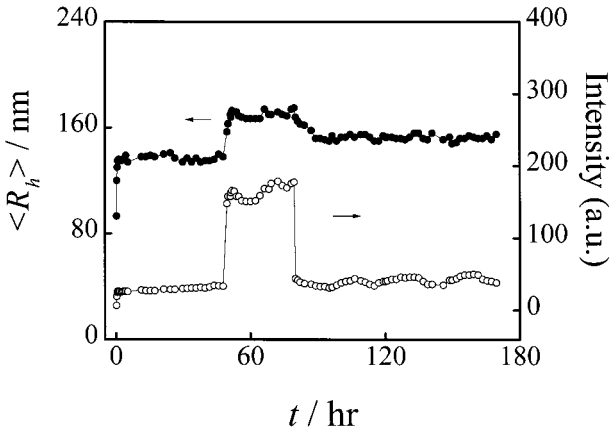

Figure 4. Incubation kinetics of the average hydrodynamic radius $\langle R_h \rangle$ and the scattered intensity for the sample dispersion with HPC concentration of 5.15×10^{-5} g/cm^3 at temperatures of 42, 44, and 42 °C.

attraction. However, the chain aggregation does not have to result in precipitation. Here, what we see is self-association of the macromolecular chains into spherical nanoparticles probably with the collapsed hydrophobic portion of macromolecular chains in their centers and as many as possible hydrophilic groups stretching into the water/particle interfaces. Obviously, with this self-assembling, the system can exist in a lower energy state, and the steric repulsion between the surface hydrophilic groups can endow the system kinetic stability. We can further speculate that the self-association of the macromolecular chains into metastable nanoparticles at the temperatures within a few degrees above the LCST is a common phenomenon. No matter what factors, such as temperature, pH, and composition, make the solvent poorer or the macromolecular chains more affinitable (by adding some other component as attraction center to form complex, for example), macromolecular chains may be able to self-associate into metastable nanospheres. In our case, it is self-association that results in steric repulsion, making the system kinetically stable.

From Figures 2 and 3 and Table 1, we can see that formation of the HPC aggregates strongly depends on temperature. We further note that even at the same temperature, HPC chains may form different metastable aggregates, depending on how the system is brought to that temperature. Once this temperature is reached, the aggregates can be very stable.

Figure 4 and Table 2 show the stability of the aggregates at 42 and 44 °C, respectively. Different from previous multistep heating, the sample cuvette was first directly put into in 42 °C index-matching vat (containing toluene as index-matching liquid) of the instrument and then heated to 44 °C along with the instrument, followed by cooling from 44 to 42 °C along with the instrument. At each temperature, the sample was allowed to stay for a relatively long time (a few days) and monitored through continuous LLS measurements. In the sudden heating from room temperature to 42 °C, both $\langle R_h \rangle$ and $\langle I_{sca} \rangle$ (average scattered intensity) quickly reached their metastable values and did not change substantially within 2 days. It worth mentioning that the stable values of both $\langle R_h \rangle$ and $\langle I_{sca} \rangle$ are smaller than those of the multistep heating (Figure 2 and Table 1), indicating the fact that the aggregates of nanoparticles were not in a thermodynamic stable but in a kinetic stable state. Interestingly, this metastable state is dependent on the most previous heating history. Sudden heating from room temperature to 42 °C led to quicker self-association of the HPC chains and the formation smaller nanoparticels. On the contrary, when the sample was incubated at intermediate temperatures in the range from 39 to 42 °C, HPC chains had more chance to associate to form larger particles. Nevertheless, the staying time at temperatures lower than 39 °C had no influence on the final particle size at 42 °C because the macromolecular chains at $T < 39$ °C were still in the coil states.

When the temperature was increased from 42 to 44 °C, both $\langle R_h \rangle$ and $\langle I_{sca} \rangle$ increased, and the aggregates reached another metastable state in about half an hour. The reorganization took longer time than it did for single chains to associate (~10 min) at 42 °C. To form larger particles with higher molar masses, the aggregates formed previously at lower temperature had to overcome the steric repulsion between the surface hydrophilic groups to contact each other for the mass transfer between them. Here again, the stable values of both $\langle R_h \rangle$ and $\langle I_{sca} \rangle$ at 44 °C are smaller than that at the same temperature when multistep heating (Figure 2 and Table 1) was used. When temperature dropped from 44 to 42 °C, the aggregates relaxed and reorganized into smaller particles in several hours. However, even after 4.5 days, $\langle R_h \rangle$ and $\langle I_{sca} \rangle$ did not go back to but reached higher stable values than that when the first time the sample was heated to 42 °C. It should be mentioned that, when further thermocycles between 44 and 42 °C were performed, the sample had repeated $\langle R_h \rangle$ and $\langle M_w \rangle$ values at 44 and 42 °C, respectively. In Figure 4, $\langle R_h \rangle$ and $\langle I_{sca} \rangle$ showed some fluctuation with time that we mainly attribute to the temperature fluctuation (due to room temperature fluctuation) in the long run measurements, as detailed in Table 2.

The formation of nanoparticle aggregates provides an ideal system for cross-linking collapsed HPC chains into gel microspheres. Two cross-linking schemes were performed using LLS sample cuvette as the reactor, and the formation of microgels has been monitored in situ by light scattering. One was to mix HPC and DVS first, heat the solution to 42 °C, and then to add NaOH into the dispersion (to reach pH ~ 12.5). The other was to mix HPC and NaOH first (to reach pH ~ 12.5), heat the solution to 42 °C, and then add DVS into the dispersion. In the second scheme, introducing NaOH greatly increased the hydrophilic interaction, leading to the formation of very large HPC aggregates ($\langle R_h \rangle \sim 330$ nm for 5.15×10^{-5} g/cm^3 HPC water dispersion). Further introducing DVS triggered cross-linking of HPC chains inside the aggregated spheres. Those spheres were so large that they tended to slowly precipitate under gravity. Finally, cross-linking between precipitated gel particles happened, resulting in a compact bulk HPC gel.

In the first scheme, the DVS (weight ratio of the DVS to the HPC being 96) was added into 5.15×10^{-5} g/cm^3 HPC water solution. Here the absolute cross-linker concentration is 0.49 wt %, while the low concentration limit of DVS for effectively cross-linking HPC is found to be about 0.15 wt %. Table 3 summarizes the change in particle size, density, and molar mass when scheme 1 was performed. The results of pure HPC chain aggregates of the same concentration are also listed for comparison. Figure 5 shows all the related particle size distribution wherein narrowly distributed nanospheres of the aggregates and gel nanoparticles were observed

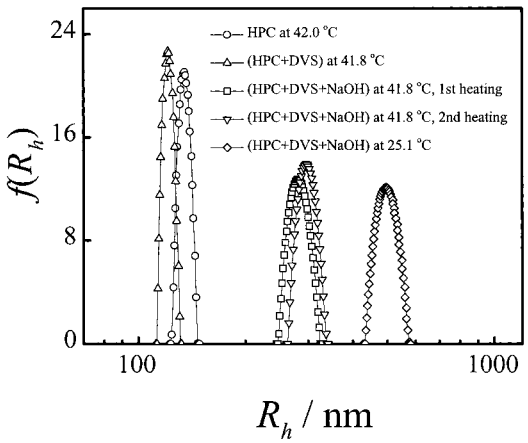

Figure 5. Hydrodynamic radius distribution of HPC aggregates and microgels in the in-situ cross-linking process. From left to right: pure HPC chains at ~42.0 °C (up triangles), mixture of HPC chains and DVS at ~41.8 °C (circles), mixture of HPC, DVS, and NaOH at ~41.8 °C (squares), the resultant microgels reheated from 25.1 to 41.8 °C (down triangles), and the resultant microgels at 25.1 °C (diamonds). The HPC concentration was 5.15×10^{-5} g/cm^3.

throughout the process. When heated to 41.8 °C, HPC chains self-associated into aggregates with similar size and molar mass as those of pure HPC aggregates without the DVS (see up triangles and circles). After incubating the dispersion at 41.8 °C for 7 h (during that period the aggregates were stable), NaOH was introduced into the sample cuvette to start cross-linking. $\langle R_h \rangle$ (squares) and $\langle M_w \rangle$ soon increased sharply, but no precipitation happened within 6 h. After cooling the system to room temperature, the particle size increased (diamonds) but the molar mass did not change, indicating the formation of the HPC gel microspheres at 41.8 °C and swelling of them at room temperature. When the dispersion was heated again to 41.8 °C, repeat $\langle R_h \rangle$ (down triangles) and $\langle M_w \rangle$ data were observed. Considering ~30% relative $\langle R_g \rangle$ error for such large chain aggregates, $\langle R_g \rangle$ does not change substantially.

Figure 6 schematically shows the conformation change of the HPC chains in the above two schemes. Although the aggregates and the gel spheres possess extremely high molar masses, static light scattering can still lead to plausible results. Figure 7 shows the Zimm plots of the pure HPC chains, the mixture of the HPC and the DVS, and the mixture of the HPC, the DVS, and NaOH at different temperatures of 40.0, 42.0, and 41.8 °C, respectively, where the concentration of the HPC was all 5.15×10^{-5} g/cm^3. For pure HPC dispersion at 40.0 and 42.0 °C (Figure 7, a and b), the linear extrapolation of $KC/R_{vv}(q)$ to the zero angle can lead to a reliable intercept value from which the apparent molar mass of the aggregates can be obtained. For the mixture of HPC−DVS and HPC−DVS−NaOH dispersions, the Zimm plots do not have the linear relationship between $KC/R_{vv}(q)$ and $(q^2 + kC)$ (Figure 7, c and d). The Berry plot, $[KC/R_{vv}(q)]^{1/2}$ vs $(q^2 + kC)$, on the other hand, can give good extrapolation results.

In more concentrated dispersions, HPC chains tend to form larger aggregates at the same temperature above the LCST. Figure 8 shows this concentration dependence on $\langle R_h \rangle$ of the aggregates. Since the aggregates are the precursors of the gel particles, it is needed to choose a suitable low concentration range to obtain narrowly distributed gel microspheres. We found that in the concentration range from 5×10^{-5} to 5×10^{-3} g/cm^3 uniform, surfactant-free microgel spheres can be obtained without stirring of the dispersions.

Conclusion

The self-association of HPC chains in water at temperatures higher than the LCST has been investigated by laser light scattering. In the narrow temperature range from 41 to 44 °C, thousands of HPC chains self-associate from dilute solution into dynamically stable nanosphere aggregates. While inter- and intrachain hydrophobic attraction is the driving force for the aggregation, the steric repulsion between hydrophilic groups of HPC chains accounts for the self-organization and the stability of the nanosphere aggregates. Enlightened by self-association of either PNIPAM or HPC chains, self-association of other neutral macromolecular chains may also be expected to occur at suitable environments. We further demonstrated that self-as-

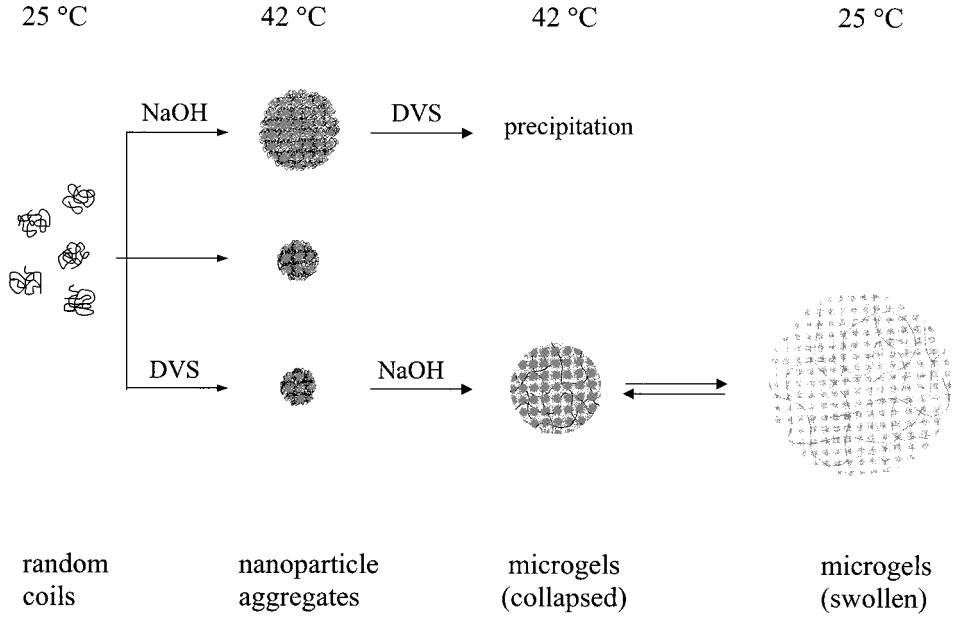

Figure 6. Schematic pictures showing conformation change HPC chains in the in situ cross-linking process at 42 °C.

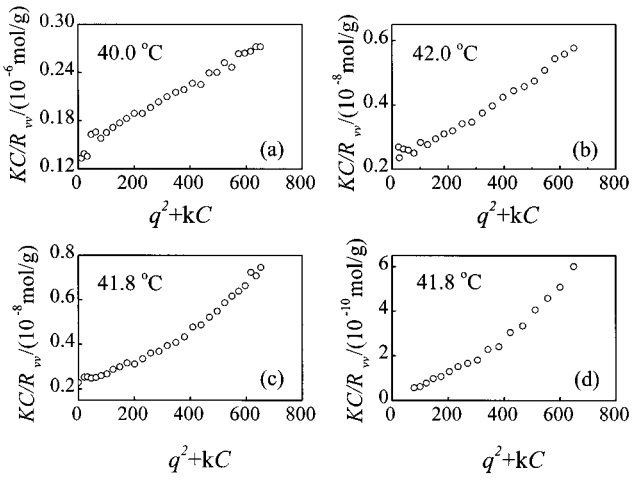

Figure 7. Angular dependence of the scattered intensity: (a) pure HPC chains at 40.0 °C; (b) pure HPC chains at 42.0 °C; (c) mixture of HPC and DVS at 41.8 °C; (d) mixture of HPC, DVS, and NaOH at 41.8 °C. The HPC concentration was 5.15 $\times$ 10^{-5} g/cm^3.

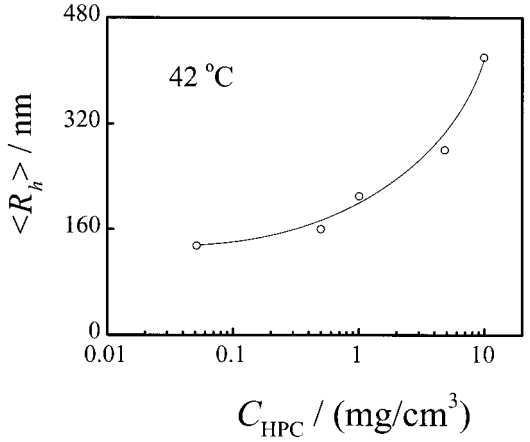

Figure 8. Concentration dependence of the average hydrodynamic radius $\langle R_h \rangle$ of HPC aggregates at 42 °C.

sociation can lead to the formation of gel microspheres by cross-linking self-associated chains.

Acknowledgment is made to the donors of the Petroleum Research Fund, administered by the American Chemical Society, and to the U.S. Army Research Office under Grant DAAG55-98-1-0175 for support of this research.

References and Notes

(1) Mortensen, K.; Brown, W.; Almdal, K.; Alami, E.; Jada, A. *Langmuir* **1997**, *13*, 3635.
(2) Mortensen, K.; Talmon, Y.; Gao, B.; Kops, J. *Macromolecules* **1997**, *30*, 6764.
(3) Mortensen, K.; Almdal, K.; Kleppinger, R.; Mischenko, N.; Reynaers, H. *Physica B* **1997**, *241*, 1025.
(4) Yu, G. E.; Yang, Z.; Attwood, D.; Price, C.; Booth, C. *Macromolecules* **1996**, *29*, 8479.
(5) Yu, G. E.; Yang, Z.; Ameri, M.; Attwood, D.; Collett, J. H.; Price, C.; Booth, C. *J. Phys. Chem. B* **1997**, *101*, 4394.
(6) Yu, G. E.; Zhou, Z. K.; Attwood, D.; Price, C.; Booth, C.; Griffiths, P. C.; Stilbs, P. *J. Chem. Soc., Faraday Trans.* **1996**, *92*, 5021.
(7) Yu, G. E.; Altinok, H.; Nixon, S. K.; Booth, C.; Alexandridis, P.; Hatton, T. A. *Eur. Polym. J.* **1997**, *33*, 673.
(8) Yu, J. M.; Jerome, R.; Teyssie, P. *Polymer* **1997**, *38*, 347.
(9) Yu, J. M.; Jerome, R. *Macromolecules* **1996**, *29*, 8371.
(10) Magnusdottir, S.; Viovy, J. L.; Francois, J. *Electrophoresis* **1998**, *19*, 1699.
(11) Liang, Y. Z.; Li, Z. C.; Li, F. M. *J. Colloid Interface Sci.* **2000**, *224*, 84.
(12) Quintana, J. R.; Hernaez, E.; Inchausti, I.; Katime, I. *J. Phys. Chem. B* **2000**, *104*, 1439.
(13) Ryu, J. G.; Jeong, Y. I.; Kim, I. S.; Lee, J. H.; Nah, J. W.; Kim, S. H. *Int. J. Pharm.* **2000**, *200*, 231.
(14) Taboada, P.; Attwood, D.; Garcia, M.; Jones, M. N.; Ruso, J. M.; Mosquera, V.; Sarmiento, F. *J. Colloid Interface Sci.* **2000**, *221*, 242.
(15) Taboada, P.; Attwood, D.; Ruso, J. M.; Garcia, M.; Sarmiento, F.; Mosquera, V. *Langmuir* **2000**, *16*, 3175.
(16) Pelton, R. H.; Chibante, P. *Colloids Surf.* **1986**, *120*, 247.
(17) Nabzar, L.; Duracher, D.; Elaissari, A.; Chauveteau, G.; Pichot, C. *Langmuir* **1998**, *14*, 5062.
(18) Wu, C; Zhou, S. Q. *Macromolecules* **1995**, *28*, 5388; **1995**, *28*, 8381.
(19) Li, M.; Wu, C. *Macromolecules* **1999**, *32*, 4311.
(20) Ding, J. F.; Liu, G. J. *Macromolecules* **1999**, *32*, 8413.
(21) Ott, E., Ed. *Cellulose and Cellulose Derivatives*; Interscience Publishers Inc.: New York, 1943.
(22) Kluc, E. D. *J. Polym. Sci.* **1971**, *36*, 491.
(23) Winnik, F. M.; Tamai, N.; Yonezawa, J.; Nishimura, Y.; Yamazaki, I. *J. Phys. Chem.* **1992**, *96*, 1967.
(24) Drummond, C.; Albers, S.; Furlong, D. N. *J. Colloids Surf.* **1992**, *62*, 75.
(25) Saunders, B. R.; Vincent, B. *Adv. Colloid Interface Sci.* **1999**, *80*, 1.
(26) Harsh, D. C.; Gehrke, S. H. *J. Controlled Release* **1991**, *17*, 175.
(27) O'Connor, S. M.; Gehrke, S. H. *J. Appl. Polym. Sci.* **1997**, *66*, 1279.
(28) Kabra, B. G.; Gehrke, S. H.; Spontak, R. J. *Macromolecules* **1998**, *31*, 2166.
(29) Sannino, A.; Esposito, A.; Nicolais, L.; Delnobile, M. A.; Giovane, A.; Balestrieri, C.; Esposito, R.; Agresti, M. *J. Mater. Sci., Mater. Med.* **2000**, *11*, 247.
(30) Lu, X.; Hu, Z.; Gao, J. *Macromolecules*, in press.
(31) Hu, Z.; Lu, X.; Gao, J.; Wang, C. *Adv. Mater.* **2000**, *12*, 1173.
(32) Chu, B. *Laser Light Scattering*, 2nd ed.; Academic Press: New York, 1991.
(33) Hormnirun, P.; Sirivat, A.; Jamieson, A. M. *Polymer* **2000**, *41*, 2127.
(34) Berne, B. J.; Pecora, R. *Dynamic Light Scattering*; Plenum Press: New York, 1976.
(35) De Gennes, P. G. *Scaling Concepts in Polymer Physics*; Cornell University Press: Ithaca, NY, 1979.
(36) Gunton, J. D.; Miguel, M. S.; Sahni, P. S. In *Phase Transitions and Phenomena*; Domb, C., Lebowitz, J. L., Eds.; Academic Press: New York, 1983; Vol. 8.
(37) Gan, Z. H.; Jim, T. F.; Li, M.; Zhao, Y.; Wang, S. G.; Wu, C. *Macromolecules* **1999**, *32*, 590.
(38) Gan, Z. H.; Jim, T. F.; Wu, C. *Polymer* **1999**, *40*, 1961.
(39) Zhao, Y.; Hu, T. J.; Lv, Z.; Wang, S. G.; Wu, C. *J. Polym. Sci., Polym. Phys.* **1999**, *37*, 3288.

MA001631G